Article

Two Genotypes of *Streptococcus iniae* Are the Causative Agents of Diseased Ornamental Fish, Green Terror Cichlid (*Aequidens rivulatus*)

Zhang Luo [1,2], Xiaohui Bai [2], Shuang Hao [2], Mengyu Wang [3], Yongjiang Wu [4] and Hanchang Sun [4,*]

[1] Tianjin Key Lab of Aqua-Ecology and Aquaculture, College of Fisheries, Tianjin Agricultural University, Tianjin 300384, China; luozhang2010@163.com
[2] Tianjin Fishery Research Institute, 442 Jiefangnan Road, Tianjin 300221, China
[3] Tianjin Institute for Food Safety Inspection Technology, 104 Xishi Road, Tianjin 300384, China
[4] Technology Innovation Center of Ecological Fishery Industrialization, College of Landscape and Life Science, Chongqing University of Arts and Sciences, Chongqing 402160, China
* Correspondence: sunhanchang199@163.com

Abstract: Green terror cichlid (*Aequidens rivulatus*) is a popular tropical freshwater ornamental fish. In 2021, an unknown disease was observed in cultured *A. rivulatus* in Tianjin, China, with a cumulative mortality rate of 25% within 7 days of onset. The main clinical signs were scale loss, skin ulceration, and slight bleeding. Histopathological observation revealed obvious damage to the liver, spleen, and kidney of diseased fish. In addition, abundant granulomas were observed in the spleen and head kidney of the diseased fish. To define the potential pathogens from *A. rivulatus*, bacteria were isolated from the visceral tissue of diseased fish with conventional methods. An artificial infection experiment was carried out to prove the pathogenicity of the isolated bacteria. The strains HG-2021-1 and HG-2021-3 were isolated from diseased fish and identified as being responsible for the disease. They were identified as *Streptococcus iniae* based on physiological and biochemical tests, *lctO* gene detection, and 16S rRNA gene sequence analysis. According to the result of multilocus sequence typing (MLST), HG-2021-1 and HG-2021-3 belong to different genotypes of *S. iniae*. Furthermore, they were found to contain the virulence genes *pgmA*, *scpI*, *cpsD*, and *pdi*, and the median lethal dose (LD$_{50}$) for *A. rivulatus* was 1.8×10^6 Colony-Forming Units (CFU)/mL and 6.6×10^6 CFU/mL, respectively. To our knowledge, this is the first report of fish coinfected by two genotypes of *S. iniae*.

Keywords: *Aequidens rivulatus*; histopathology; *Streptococcus iniae*; genotypes

Key Contribution: This is the first report of fish coinfected by two genotypes of *S. iniae*, and of *S. iniae*-induced visceral nodules in fish.

1. Introduction

Ornamental fish production is a thriving industry that has witnessed significant growth resulting from the increasing demand driven by improved living standards. Compared with edible fish, ornamental fish offer higher economic value and profitability. China is a leading country in terms of ornamental fish farming, with a production value of CNY 9.486 billion in 2021 [1]. The green terror cichlid *Aequidens rivulatus* (Cichlidae) is an ornamental fish originating from South America. In 1999, it was introduced to China and quickly gained popularity among ornamental fish enthusiasts because of its vibrant colors and adaptability. It is now one of the primary species of tropical freshwater ornamental fish in China [2]. However, with the increase in aquaculture density and the deterioration of water environments, disease outbreaks have become a major bottleneck hindering its development. To date, there have been relatively few studies of diseases affecting *A. rivulatus*, with reports primarily focusing on the bacterial pathogens *Streptococcus agalactiae*, *Citrobacter freundii*, *Aeromonas caviae*, and *Aeromonas veronii* [3,4].

In July 2021, a disease outbreak occurred in *A. rivulatus* at a fish farm located in Tianjin Municipality, with a cumulative mortality rate that reached 25% within 7 days after the disease was first reported. The diseased *A. rivulatus* showed anorexia, lethargy, swimming abnormalities, loss of balance, and spinning around in the water. In the present study, we investigated the cause of this disease by sampling diseased fish for bacterial isolation, pathology, physiological and biochemical features, and 16s rDNA sequence analysis. Our results are significant for the development of guidance for the prevention and treatment of diseases affecting *A. rivulatus*.

2. Materials and Methods

2.1. Fish

In July 2021, an unknown disease was observed in cultured *A. rivulatus* in Jinnan district, Tianjin Municipality, with a cumulative mortality rate of 25% ~7 days after the disease was first reported. Thirty thousand fish (body weight 62.9 ± 16.2 g) were farmed in ten tanks. They were 45 M^2 in area containing 54,000 L water, and the stocking density was 6 tails per 100 L water. No filter apparatus or sterilizing measures were used. One-fourth of the water was changed twice a day. The water temperature, dissolved oxygen, and pH recorded during the outbreaks were 28 °C, 5.6 mg L^{-1}, and 8.2, respectively. Nine samples of fish with symptoms typical of the disease (body weight 43.3–89.5 g) were loaded into oxygen bags and quickly sent to the laboratory for diagnosis.

2.2. Bacterial Isolation and Parasite Check

After being euthanized by an overdose of tricaine methanesulphonate (MS222), each diseased *A. rivulatus* was wiped several times with 75% ethanol-saturated cotton. Each fish was then dissected under aseptic conditions and the liver, spleen, and kidney were scored onto Brain Heart Infusion (BHI) agar, thiosulfate–citrate–bile salts–sucrose agar (TCBS), and 7H10 agar supplemented with oleic acid, albumin, dextrose, and catalase (OADC) plates. The plates were cultured for 3 days at 28 °C. Dominant colonies were selected for bacterial purification. In addition, samples of mucus, gill, fins, and visceral tissue from three diseased fish were examined under a microscope for parasites.

Samples of spleen, liver, head kidney, and kidney from three diseased fish were cut into 1~2 mm^3 portions and fixed in 2.5% glutaraldehyde. After ethanol dehydration, the samples were embedded in Epon812 resin, sectioned using a conventional approach, and stained with uranyl acetate. The samples were observed under a transmission electron microscope (TEM) and photographed.

2.3. Pathological Section

The liver, kidney, head kidney, spleen, and heart were removed from three diseased *A. rivulatus* and fixed in 10% neutral buffered formalin. Fixed tissues were processed by routine histological procedures; 5 μm thick tissue sections were stained with hematoxylin and eosin (H&E) and Ziehl–Neelsen staining (Z&N). Tissues from three healthy *A. rivulatus* were processed using the same methodology and served as controls.

2.4. Specific Pathogen Detection for Disease Fish

Samples of spleen, liver, and kidney were mixed from three diseased fish, and the genomic DNA was extracted using the Genomic DNA extraction kit (SBS, Shanghai, China) according to the manufacturer's protocol. The genomic DNA was used to detect pathogens including *Mycobacterium* spp., *Renibacterium salmoninarum*, *Rickettsia*-like organisms, *Nocardia seriolae*, and *Francisella* spp. by PCR according to a previously published method (Table 1).

Table 1. PCR primers used in this study.

Primer	Sequence (5′–3′)	Length (bp)	Application
T39 T13	GCGAACGGGTGAGTAACACG TGCACACAGGCCACAAGGGA	936	Test *Mycobacteria* spp. by nested PCR [5]
preT43 T531	AATGGGCGCAAGCCTGATG ACCGCTACACCAGGAAT	300–312	
P3 M21	AGCTTCGCAAGGTGAAGGG GCAACAGGTTTATTTGCCGGG	383	Test *R. salmoninarum* by nested PCR [6]
P4 M38	ATTCTTCCACTTCAACAGTACAAGG CATTATCGTTACACCCGAAACC	320	
PS-F PS-R	CTAGGAGATGAGCCCGCGTTG ATTTCA CATCCAACTTAATCT	390	Test Piscirickettsia by PCR [7]
Noc-f Noc-r	CACCTACGAAAATCCCATTTGGT CATCGGATTGGATTCAAGGACCTTGA	156	Test *Nocardia seriolae* by PCR [8]
F5 F11	CCTTTTTGAGTTTCGCTCC TACCAGTTGGAAACGACTGT	1133	Test *Francisella* spp. by PCR [9] (FORSMAN)
lctO-F lctO-R	AAGGGGAAATCGCAAGTGCC ATATCTGATTGGGCCGTCTAA	870	Clone *lctO* gene [10]
27F 1492R	AGAGTTTGATCCTGGCTCAG TACGGCTACCTTGTTACGCTT	1480–1494	Clone 16S rRNA gene [11]
dnaN-F dnaN-R	GCACATGTTAATTCGCCAGAGG CAGCACCAACTCTGATAATTTTCCA	404	Multilocus sequence typing [12]
mutL-F mutL-R	CCAACCAAGCAGGAAGTTCG CGTTCTTGAGCTGCGTGTTG	545	
mutM-F mutM-R	CAGAGTAGATGGTTTGACCC TGCCCTGTATGATGCCTATC	410	
mutS-F mutS-R	TTTAACTGGCGCATCCCCAT TGGATCTTGCAACAGGTGAGT	448	
mutX-F mutX-R	TGGCCATTGGTTTCATCAAGG CGTAATCCCCTTCCCACGTT	547	
recD2-F recD2-R	AGGGCTTCCTAGTGCTACCA ACTCGCTTTGCCCATCAAGA	563	
rnhC-F rnhC-R	GGAATCGCTGTTGTTGCAAGT TTGAGTGTTTGCGAAGTGGC	582	
yfhQ-F yfhQ-R	AGGCCAGGTGATTTCAACCA CAGGAGAAACCCAGGCCATT	511	
pgmA-F pgmA-R	AGACGGGGTCACAGACTACAT AGGAGCACTTTGACGGAATT	949	Test virulence genes by PCR [13,14]
cfi-F cfi-R	GTGCCTCAACATCAAACA TAGCAAATCCCATATCAA	328	
scpI-F scpI-R	GCAACGGGTTGTCAAAAATC GAGCAAAAGGAGTTGCTTGG	822	
simA-F simA-R	AATTCGCTCAGCAGGTCTTG AACCATAACCGCGATAGCAC	994	
pdi-F pdi-R	TTTCGACGACAGCATGATTG GCTAGCAAGGCCTTCATTTG	381	
sagA-F sagA-R	AGGAGGTAAGCGTTATGTTAC AAGAAGTGAATTACTTTGG	190	
cpsD-F cpsD-R	TGGTGAAGGAAAGTCAACCAC TCTCCGTAGGAACCGTAAGC	534	

2.5. Physiological and Biochemical Features

Purified single colonies were streaked on Brain Heart Infusion agar (BHI) and tryptone soy agar (TSA) containing 5% sheep blood to enable observations of colony morphology. The isolated strains were then subjected to physiological and biochemical tests using the

method developed by Dong and Cai, including Gram staining, motility, hemolysis, methyl red reaction, and so on [15].

2.6. Lactate Oxidase-Encoding (lctO) and 16S rRNA Gene Sequence Analysis

The genomes of isolates HG-2021-1, HG-2021-3, and *S. iniae* ATCC 28179 were extracted, and PCR amplification of the *lctO* and 16S rRNA genes was performed using the primers in Table 1 in 50 µL PCR reaction mixture, containing 1 µL of each primer (10 µM), 2 µL template, 21 µL H_2O, and 25 µL Premix Taq™ (TaKaRa, Dalian, China), in the C1000 ™ Thermal Cycler (Bio-Rad, Hercules, CA, USA), with an initial denaturation cycle of 95 °C for 5 min, then 35 cycles of 95 °C for 30 s, 55 °C for 30 s, 72 °C for 90 s, and then a final extension of 72 °C for 10 min. After being purified, the amplified products were sequenced by Sangon Biotech (Shanghai, China). The sequencing results of 16S rRNA genes were aligned and compared for homology with gene fragments in the National Center for Biotechnology Information (NCBI) GenBank using Basic Local Alignment Search Tool (BLAST) (http://www.ncbi.nlm.nih.gov/blast/ accessed on 3 February 2024). Multiple alignment of 16S rRNA sequences from related *Streptococcus*-type strains and isolates available on GenBank, construction of a phylogenetic tree by the neighbor-joining method, and 1000-replicate bootstrap analysis for the evaluation of phylogenetic tree topology were carried out with MEGA version 4.1 software [16,17]. Evolutionary distances were calculated using the Kimura two-parameter model [18].

2.7. Multilocus Sequence Typing (MLST)

Eight loci or housekeeping genes, including *dnaN, rnhC, yfhQ, recD2, mutM, mutX, mutL,* and *mutS*, were selected for MLST analysis using a previously published method [12,19]. By using the genomes of HG-2021-1 and HG-2021-3 as templates, the eight genes were amplified by PCR using specific primers (Table 1), and the amplified products were sequenced by Sangon Biotech (Shanghai). The gene sequences were analyzed using an online comparison tool (https://pubmlst.org/bigsdb?db=pubmlst_siniae_seqdef accessed on 1 April 2024) to determine the sequence numbers of the *dnaN, rnhC, yfhQ, recD2, mutM, mutX, mutL,* and *mutS* genes, and the corresponding sequence type (ST).

2.8. PCR Tests of Virulence Genes

By using the genome of HG-2021-1, HG-2021-3, and *S. iniae* ATCC 28179 as templates, PCR amplification was performed on C5a peptidase (*scpI*), SiM protein (*simA*), phosphoglucomutase (*pgmA*), capsular polysaccharide (*cpsD*), streptolysin S-associated protein (*sagA*), polysaccharide deacetylase (*pdi*), and CAMP factor (*cfi*) genes according to previous methods [13,14].

2.9. Artificial Infection

Strains HG-2021-1 and HG-2021-3 were selected for the infection test in which 270 healthy *A. rivulatus* (22.5 ± 3.6 g) were acclimated in the laboratory for 2 weeks. They were then arbitrarily divided into nine groups (n = 30) and placed in 45 L aquaria containing 35 L dechlorinated water. Water temperature, pH, dissolved oxygen, oxygen saturation value, and electric conductivity were 27–28 °C, 7.6–7.8, 6.1–8.3 mg/L, 76.3–103.9%, and 175 µS/cm–204 µS/cm, respectively. Group 1 was injected intraperitoneally with 0.1 mL PBS (pH 7.4) as the control group. Groups 2–5 were injected with 0.1 mL of 3.3×10^8, 10^7, 10^6, and 10^5 CFU/mL of a tenfold serial dilution of the HG-2021-1 suspension, respectively, and groups 6–9 were injected with the same volume and the same concentration of the HG-2021-3 suspension. The test fish were continuously observed for 14 days; any morbid fish were removed quickly and used for re-isolation of the pathogens. The mortality rate was determined and LD_{50} was calculated. Furthermore, spleens and kidneys removed from three dying fish infected by different strains were used for pathological evaluation.

2.10. Antimicrobial Susceptibility Testing

The antimicrobial susceptibility patterns of the HG-2021-1 and HG-2021-3 isolates were tested using a previously published method [20]. Briefly, 0.1 mL of a 10^8 CFU/mL HG-2021-1 and HG-2021-3 suspension was plated onto Mueller Hinton agar supplemented with 5% fetal bovine serum (FBS). The plates were left for 5 min, and then drug-sensitive test papers including ampicillin, chloromycetin, streptomycin, norfloxacin, kanamycin, doxycycline, enoxacin, gentamycin, ciprofloxacin, erythromycin, roxithromycin, tetracycline, florfenicol, vancomycin, and tobramycin purchased from Hangzhou microbial reagent Co., Ltd. (Hangzhou, China) were added. The plates were then cultured for 48 h at 28 °C. The sensitivity of HG-2021-1 and HG-2021-3 to the test drugs was determined based on the diameter of the inhibition zone on each plate. According to the instructions provided by the manufacturer, the results were classified as sensitive (S), intermediate sensitive (I), and resistant (R).

3. Results

3.1. Clinical Signs and Pathological Features

Diseased fish showed a loss of scales, skin ulceration, and petechial hemorrhages (Figure 1A). Upon dissection, a small amount of fluid accumulation in the coelomic cavity and transparent intestinal walls were observed. The most notable feature was the presence of numerous nodules in the spleen (Figure 1B). Pathological examination revealed blood cell congestion in the diseased fish liver, accompanied by hepatocyte vacuolation, swelling, and necrosis (Figure 2B). Oval nodules were found in the spleen and head kidney, with a higher quantity in the spleen, some of which were interconnected (Figure 2D,E,H). The spleen exhibited a decreased red blood cell count and extensive cell necrosis (Figure 2D,E). Many macrophages were observed in the outer layer of the nodules in the head kidney (Figure 2H). Also, in the kidneys, granular degeneration and necrosis of the renal tubular epithelial cells were observed (Figure 2G). No pathological changes were found in the heart. Furthermore, small nodules were found in the spleen of the fish infected artificially (Figure 2I).

Figure 1. *Aequidens rivulatus* showing typical symptoms of disease. (**A**) A loss of scales, skin ulceration, and slight bleeding; (**B**) abundant white granulomas in the spleen (→), and transparent intestinal walls (★).
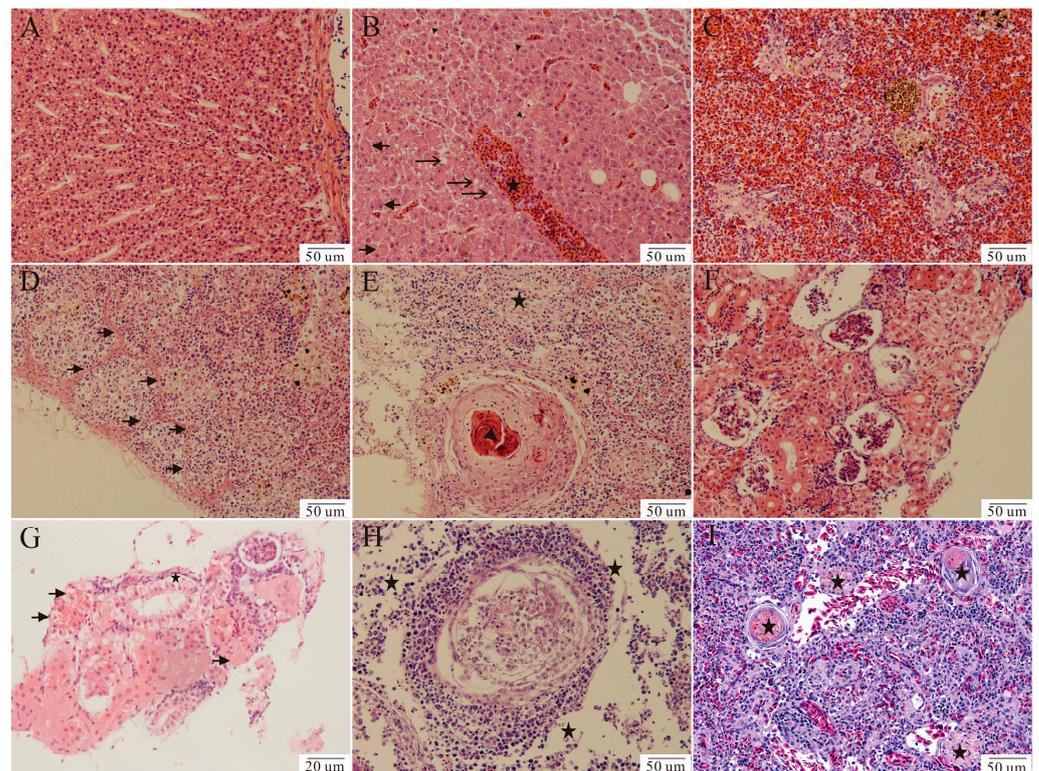
Figure 2. Histological sections of the organs of diseased *Aequidens rivulatus*. (**A,C,F**) Liver, spleen, and kidney of disease-free *A. rivulatus* for comparison. (**B**) Liver, showing hepatocyte vacuolation (→), swelling (➤), necrosis (◀), and accumulation of red blood cells (★). (**D**) Spleen, showing oval nodules interconnected by fibroblasts (➤). (**E**) Spleen, showing granulomas characterized by necrotic centers surrounded by a thin fibrous capsule (◀), a decreased number of red blood cells, and extensive cell necrosis (★). (**G**) Kidney, showing renal tubular epithelial cell granular degeneration (➤) and necrosis (★). (**H**) Anterior kidney, showing extensive cell necrosis (★), and many macrophages in the outer layer of the granuloma. (**I**) Spleen from the fish artificially infected with strain HG-2021-1, showing small circular nodules (★).

3.2. Specific Pathogen Detection in Diseased Fish and Isolation of Pathogenic Bacteria

Except for a few triehodinids in the gill filaments and mucus of the body surface, no other parasites were observed on other parts of the body with either the naked eye or a light microscope. In addition, no virus particles were observed in the gills, spleen, and kidney tissues during TEM.

PCR was used to detect the presence of *Mycobacterium* spp., *Renibacterium salmoninarum*, *Rickettsia* spp., *Nocardia seriolae*, and *Francisella* spp., but the results were negative (results not shown). No bacterium grew on TCBS or 7H10 plates; however, numerous colonies including two different colony morphologies were observed on BHI agar plates, both exhibiting gray circular colonies of varying sizes. One kind of colony was larger, with a diameter of 0.6–0.8 mm, whereas the other was smaller, with a diameter of 0.2–0.3 mm. These colonies were purified and named HG-2021-1 and HG-2021-3, respectively. HG-2021-1 exhibited uniform turbid growth, whereas HG-2021-3 exhibited sedimentary growth with transparent liquid and a white precipitate at the bottom (Figure 3).

Figure 3. The morphology of strains HG-2021-1 and HG-2021-3 cultured in the liquid culture medium BHI. (**A**) Strain HG-2021-1, showing uniform turbid growth. (**B**) Strain HG-2021-3, showing sedimentary growth with transparent liquid and a white precipitate at the bottom.

3.3. Identification of Isolated Strains

The physiological and biochemical characteristics of the colonies are summarized in Table 2. Both colonies showed Gram-positive cocci arranged in chains or pairs, with characteristics including no motility and α-type hemolysis. The strains were also capable of utilizing glucose, trehalose, maltose, and sucrose, but not mannitol or sorbitol. Furthermore, they showed positive results in methyl red tests, arginine dihydrolase, and esculin hydrolysis. Furthermore, the results showed little difference between strains HG-2021-1 and HG-2021-3. Strain HG-2021-1 showed positive results in phosphatase and negative results in amygdalin, xylose, and raffinose tests, while strain HG-2021-3 was the opposite (Table 2).

Table 2. Physiological and biochemical characteristics of isolated strains.

Items	HG-2021-1	HG-2021-3	Items	HG-2021-1	HG-2021-3
Gram stain	+	+	Vogus–Proskauer	−	−
10 °C growth	−	−	Catalase	−	−
45 °C growth	−	−	Methyl red reaction	+	+
Motility	−	−	Esculin hydrolysis	+	+
Mannitol	−	−	Sucrose	+	+
Glucose	+	+	6.5% NaCl growth	−	−
Sorbitol	−	−	Glucose gas production	−	−
Oxidase	−	−	Hemolysis	α	α
Urease	−	−	Arginine dihydrolase	+	+
D-trehalose	+	+	D-maltose	+	+
a-galactosidase	−	−	β-glucuronidase	+	+
Phosphatase	+	−	D-raffinose	−	+
D-amygdalin	−	+	D-xylose	−	+

Note: "+" represents positive reaction results; "−" represents negative reaction results; "α" represents α-type hemolysis.

PCR amplification of partial *lctO* gene sequences of HG-2021-1, HG-2021-3, and *Streptococcus iniae* ATCC 28179 yielded fragments of 870 bp (Figure 4). Sequence assays showed that they displayed the same nucleotide sequence. PCR amplification of partial 16S rRNA gene sequences of HG-2021-1 (GenBank no. PP492817) and HG-2021-3 (GenBank no. PP495151) yielded fragments of ~1500 bp. Alignment analysis using the NCBI database showed high homology (99.7%) with *S. iniae* ATCC 29178 (GenBank no. NR115731). Phylogenetic analysis revealed that the 16S rRNA gene sequences of HG-2021-1 and HG-2021-3 also clustered with *S. iniae* (Figure 5). Based on the result of *lctO* gene detection, 16S rRNA gene sequence analysis, and physiological and biochemical reactions, both HG-2021-1 and HG-2021-3 were identified as *S. iniae*.
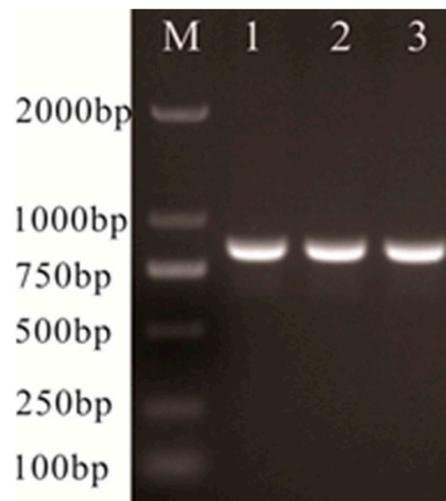
Figure 4. PCR tests of *lctO* genes. M: DL2000 DNA marker; lanes 1, 2, and 3 indicate tests of isolates HG-2021-1, HG-2021-3, and *Streptococcus iniae* ATCC 28179.
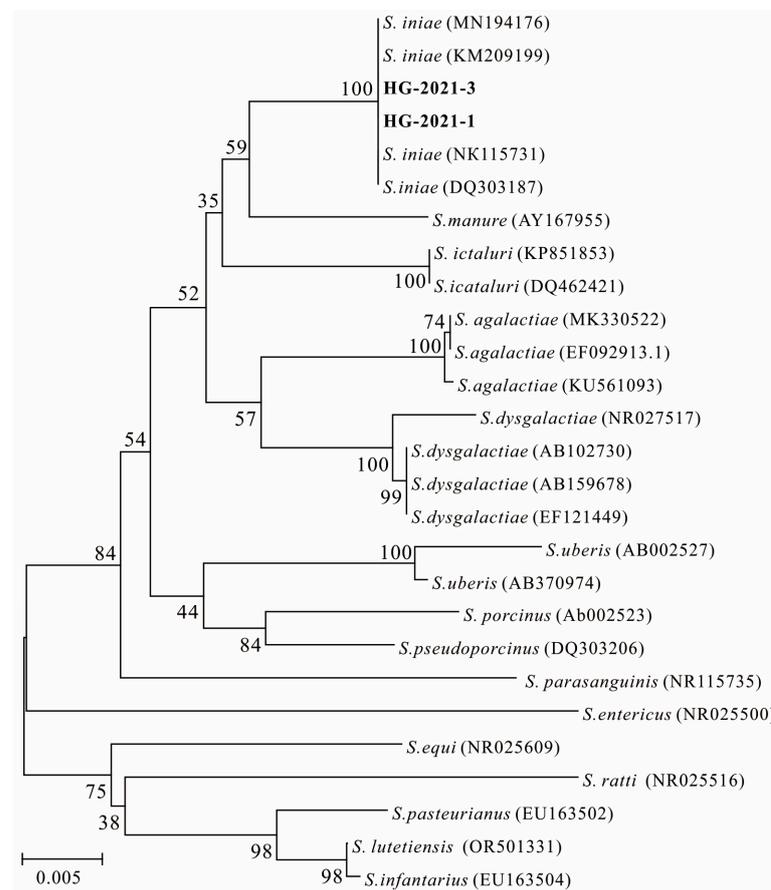

Figure 5. Phylogenetic tree constructed for strains HG-2021-1 and HG-2021-3 based on the 16S rRNA gene sequences of related *Streptococcus* spp. GenBank accession numbers are given in parentheses.

3.4. MLST

MLST analysis of the HG-2021-1 strain suggested that the corresponding sequence numbers of the *dnaN*, *rnhC*, *yfhQ*, *recD2*, *mutM*, *mutX*, *mutL*, and *mutS* genes were 1, 1, 1, 1, 1, 1, 1, and 1, respectively, with the corresponding sequence type (ST) being 4. Similarly, the sequence numbers of the eight genes in the HG-2021-3 strain were 4, 4, 2, 2, 3, 4, 2, and 3, respectively, with the corresponding sequence type (ST) being 1.

3.5. Detection of Virulence-Related Genes

Using HG-2021-1, HG-2021-3, and *Streptococcus iniae* ATCC 28179 as templates, PCR amplification was performed on the virus genes *scpI*, *simA*, *pgmA*, *cpsD*, *sagA*, *pdi*, and *cfi*. The amplification results showed that target bands of corresponding sizes were obtained for *pgmA*, *scpI*, *cpsD*, and *pdi*. The target fragment was not obtained for *cfi*, *simA*, or *saga* (Figure 6).
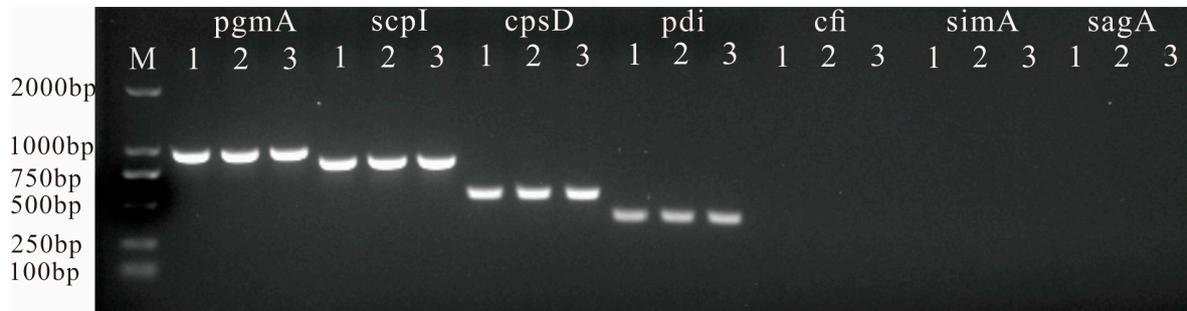

Figure 6. PCR tests of virulence genes *scpI*, *simA*, *pgmA*, *cpsD*, *sagA*, *pdi*, and *cfi*. M: DL2000 DNA markers; lanes 1, 2, and 3 indicate isolates *Streptococcus iniae* ATCC 28179, HG-2021-1, and HG-2021-3.

3.6. Artificial Infection

Two days after artificial infection, fish in the experimental group exhibited symptoms of anorexia and buoyancy disorders, whereas the control group showed no such signs. From the third day after artificial infection, fish began to die. After 14 days, the cumulative mortality of *A. rivulatus* in groups 2–5 was 100%, 93.3%, 60.0%, and 23.3%, respectively, and 90%, 70%, 43.3%, and 13.3% in groups 6–9, respectively. The LD$_{50}$ of strain HG-2021-1 and HG-2021-3 was 1.8×10^6 CFU/mL and 6.6×10^6 CFU/mL, respectively (Table 3). The main symptoms observed in the dead fish included abdominal distension, the presence of ascites, and hemorrhagic spots on the body surface, similar to those observed in naturally diseased fish. The bacterial strains isolated from the affected fish internal organs exhibited the same physiological and biochemical characteristics, as well as 16S rRNA gene sequences, as HG-2021-1 and HG-2021-3.

Table 3. Experimental infection with isolates HG-2021-1 and HG-2021-3 in *Aequidens rivulatus*.

Isolates	Bacterial Concentration (CFU/mL)	Amount of Death Post-Infection in Different Days														Cumulative Mortality (%)	LC$_{50}$ (CFU/mL)
		1	2	3	4	5	6	7	8	9	10	11	12	13	14		
HG-2021-1	3.3×10^8	0	0	5	8	12	18	26	30	30	30	30	30	30	30	100	1.8×10^6
	3.3×10^7	0	0	3	6	11	18	24	27	28	28	28	28	28	28	93.3	
	3.3×10^6	0	0	1	6	8	12	15	16	17	18	18	18	18	18	60.0	
	3.3×10^5	0	0	0	0	1	2	4	6	6	7	7	7	7	7	23.3	
HG-2021-3	3.1×10^8	0	0	4	5	8	14	23	27	27	27	27	27	27	27	90.0	6.6×10^6
	3.1×10^7	0	0	3	3	7	7	11	12	14	21	21	21	21	21	70.0	
	3.1×10^6	0	0	1	2	4	7	8	8	10	11	13	13	13	13	43.3	
	3.1×10^5	0	0	0	0	1	2	2	3	3	3	4	4	4	4	13.3	
PBS		0	0	0	0	0	0	0	0	0	0	0	0	0	0	0	0

3.7. Antibiotic Susceptibility Test

The antibiotic susceptibility test demonstrated that strain HG-2021-1 was consistent with HG-2021-3. Both were sensitive to streptomycin, ampicillin, florfenicol, roxithromycin, and erythromycin, but resistant to neomycin, polymyxin B, doxycycline, tobramycin, levofloxacin, norfloxacin, ciprofloxacin, vancomycin, and gentamycin (Table 4).

Table 4. Sensitivity of strains HG-2021-1 and HG-2021-3 to 16 different antibiotics.

Antibiotics	Sensitivity		Antibiotics	Sensitivity	
	HG-2021-1	HG-2021-3		HG-2021-1	HG-2021-3
Tetracycline	I	I	Ampicillin	S	S
Neomycin	R	R	Norfloxacin	R	R
Streptomycin	S	S	Ciprofloxacin	R	R
Polymyxin B	R	R	Florfenicol	S	S
Doxycycline	R	R	Vancomycin	R	R
Kanamycin	I	I	Roxithromycin	S	S
Tobramycin	R	R	Gentamycin	R	R
Levofloxacin	R	R	Erythromycin	S	S

Note: "S": sensitive; "I": intermediate sensitive; "R": resistant.

4. Discussion

In recent years, the formation of granulomas in visceral tissues has been reported in various marine and freshwater fish, such as turbot *Scophthalmus maximus*, half-smooth tongue sole *Cynoglossus semilaevis* Günther, seahorse *Hippocampus erectus*, and largemouth bass *Micropterus salmoides* [21–25]. Parasites, viruses, and bacteria have been identified as potential causes of nodules of internal organs in fish [26,27]. In our study, no parasites or viral particles were observed in the tissues of diseased fish exhibiting nodular symptoms, ruling out the possibility of parasitic or viral infections. It has been reported that bacteria such as *Mycobacterium* spp., *Nocardia seriolae*, *Renibacterium salmoninarum*, *Rickettsia* spp., *Francisella* spp., *Photobacterium damselae*, *Aeromonas schubertii*, and *Aeromonas salmonicida* can cause nodules of internal organs in fish [21–25,28–31]. PCR detection of the first five pathogens was used in the current study, but yielded negative results. These results ruled out the possibility of the diseased fish being infected by *Mycobacterium* spp., *R. salmoninarum*, *Nocardia seriolae*, *Francisella* spp., or *Rickettsia* spp.

Two different bacterial strains with distinct colony sizes were isolated from the internal organs of the affected fish using a BHI agar medium. Artificial infection experiments revealed that both strains were pathogenic to *A. rivulatus*, with experimentally infected fish exhibiting symptoms similar to those observed in naturally infected fish, indicating that they were the causative agents of the disease impacting *A. rivulatus*. Upon identification, both strains were identified as *S. iniae*.

Although *S. iniae* is phenotypically well characterized, laboratory identification can be difficult, especially when using commercial identification systems, because no currently available commercial system includes *S. iniae* in its database [10]. In this paper, *lctO* and 16S rRNA gene sequence analyses were performed. Based on these experimental results, strains HG-2021-1 and HG-2021-3 were identified as *S. iniae.*

Strains HG-2021-1 and HG-2021-3 exhibited significant differences in physiological and biochemical characteristics. This suggests that they may belong to different genotypes, and the hypothesis has been confirmed by MLST. Additionally, HG-2021-3 exhibited a higher LD_{50} in fish, indicating weaker virulence compared with HG-2021-1. This finding is consistent with that of Kim et al., who reported that two genotypes of *S. iniae* showed different virulence [32].

S. iniae is a major pathogen in many fish species, including freshwater fish, such as sturgeon *Acipenser transmontanus* L., tilapia *Oreochromis* spp., and channel catfish *Ictalurus punctatus*, and marine fish, as such red porgy *Pagrus pagrus* L. and small yellow croaker *Larimichthys polyactis*, causing severe economic losses [33–38]. We also isolated *S. iniae* from affected silver scat *Selenotoca multifasciata* in nearby fish farms, indicating that *S. iniae* is a common pathogen in the aquaculture of the region [39]. However, we did not observe nodular symptoms in the visceral tissues of silver scat. This might indicate that the formation of visceral nodules is not only pathogen- but also fish species-dependent. This finding is consistent with that of Luo et al., who reported that artificial infection of four different species of fish with *Nocardia seriolae* resulted in nodules that appeared on day 5

post-infection in *Micropterus salmoides* and *Channa argus*, whereas no nodules were observed in *Ctenopharyngodon idella* or *Oreochromis niloticus* even after 14 days of infection [40]. The identification of drugs that *S. iniae* was susceptible to indicates these could be used to treat infected fish. However, the formation of nodules can hinder drug penetration, thereby affecting the efficacy of drug treatment. To improve treatment outcomes and minimize economic losses caused by *S. iniae*. it is crucial for farmers to enhance their observation of cultured organisms, promptly detect diseases, and administer treatment with sensitive drugs before nodule formation.

5. Conclusions

In conclusion, two genotypes of *S. iniae* were isolated from diseased *A. rivulatus* and were believed to be the pathogenic agents; pathologic characteristics were observed, and five sensitive drugs were screened. The results provide a foundation for the development of guidance for the prevention and treatment of diseases affecting *A. rivulatus*.

Author Contributions: Z.L.: investigation, data curation, writing—review and editing. X.B.: formal analysis, writing—original draft preparation. S.H.: methodology, formal analysis. M.W.: software, literature comparative dialogue. Y.W.: software, literature comparative dialogue. H.S.: writing—review and editing, project administration, and funding acquisition. All authors have read and agreed to the published version of the manuscript.

Institutional Review Board Statement: All animal experiments were approved and conducted in compliance with all experimental practices and standards developed by the Animal Welfare and Research Ethics Committee of Tianjin Agricultural University.

Data Availability Statement: All the data generated or used during the study appear in the submitted article.

Conflicts of Interest: The authors declare that there are no conflicts of interest regarding the publication of the work described in this manuscript.

References

1. Yu, X.J.; Hao, X.J.; Yang, L.K.; Dang, Z.Q. Development monitoring report of Chinese recreational fishery. *China Fish.* **2022**, *12*, 35–40.
2. Wu, J.; Gao, Q.; Yang, H.; Yang, G.L. Artificial propagation and seed cultivation technology of green terror cichlid *Aequidens rivulatus*. *Fish. Sci. Technol. Info.* **2012**, *39*, 171–173.
3. Yao, X.L.; Xu, X.L.; Li, H.M.; Zhong, W.H.; Zang, L.; Li, H.; Yang, C.J. Biological characteristics of pathogenic *Streptococcus agalactiae* isolated from *Aequidens rivulatus*. *Prog. Fish. Sci.* **2015**, *36*, 106–112.
4. Hao, X.B.; Huang, Y.P.; Hu, Q.; Peng, Y.O.; Sun, L.M.; Gao, J.W.; Song, R. Pathogen isolation, identification and drug susceptibility analysis of *Aequidens rivulatus* hole-in-the-head disease. *Curr. Fish.* **2021**, *6*, 60–63.
5. Talaat, A.M.; Reimschuessel, R.; Trucksis, M. Identification of mycobacteria infecting fish to the species level using polymerase chain reaction and restriction enzyme analysis. *Vet. Microbiol.* **1997**, *58*, 229–237. [CrossRef]
6. Chase, D.M.; Pascho, R.J. Development of a nested polymerase chain reaction for amplification of a sequence of the p57 gene of *Renibacterium salmoninarum* that provides a highly sensitive method for detection of the bacterium in salmonid kidney. *Dis. Aquat. Org.* **1998**, *3*, 223–229. [CrossRef]
7. Lei, Y.; Zhang, H.J.; Wang, J.; Zhang, W.E.; Tang, S.L.; Xiao, Y.; Wang, X.P. Development and Primary Application of a PCR Assay for Detection of *Piscirickettsia*-like Organisms. *J. Guangdong Ocean Univ.* **2015**, *35*, 30–34.
8. Jiang, Y.Y.; Li, A.X. Establishment of a specific PCR assay to detect *Nocardia seriolae*. *S. China Fish. Sci.* **2011**, *7*, 47–51.
9. Forsman, M.; Sandstrom, G.; Sjostedt, A. Analysis of 16s ribosomal DNA sequences of *Francisella* strains and utilization for determination of the phylogeny of the genus and for identification of strains by PCR. *Int. J. Syst. Bacteriol.* **1994**, *44*, 38–46. [CrossRef]

10. Mata, A.I.; Blanco, M.M.; Dominguez, L.; Fernandez-Garayzabal, J.F.; Gibello, A. Development of a PCR assay for *Streptococcus iniae* based on the lactate oxidase (*lctO*) gene with potential diagnostic value. *Vet. Microbial.* **2004**, *101*, 109–116. [CrossRef]

11. Lane, D.J. 16S/23S rRNA sequencing. In *Nucleic Acid Techniques in Bacterial Systematics*; Stackebrandt, E., Goodfellow, M., Eds.; Wiley: New York, NY, USA, 1991.

12. Irion, S.; Rudenko, O.; Sweet, M.; Chabanet, P.; Barnes, A.C.; Tortosa, P.; Séré, M.G. Molecular investigation of recurrent *Streptococcus iniae* epizootics affecting coral reef fish on an oceanic island suggests at least two distinct emergence events. *Front. Microbial.* **2021**, *12*, 749734. [CrossRef]

13. Xiong, X.Y.; Huang, G.Q.; Wang, Z.C.; Wen, X. Molecular typing, antibiogram type and detection of virulence genes of *Stereptococcus iniae* strains isolated from golden pompano (*Tranchinotus ovatus*) in Guangxi province. *J. Fish. China* **2018**, *42*, 586–595.

14. Baums, C.G.; Hermeyer, K.; Leimbach, S.; Adamekk, M.; Czerny, C.P.; Horstgen-Schwark, G.; Valentin-Weigand, P.; Baumgartner, W.; Steinhagen, D. Establishment of a Model of *Streptococcus iniae* Meningoencephalitis in Nile Tilapia (*Oreochromis niloticus*). *J. Comp. Path.* **2013**, *149*, 94–102. [CrossRef] [PubMed]

15. Dong, X.Z.; Cai, M.Y. *Manual of Familiar Bacterium Identification*; Science Press: Beijing, China, 2001.

16. Saitou, N.; Nei, M. The neighbor-joining method: A new method for reconstructing phylogenetic trees. *Mol. Biol. Evol.* **1987**, *4*, 406–425. [PubMed]

17. Tamura, K.; Battistuzzi, F.U.; Billing-Ross, P.; Murillo, O.; Filipski, A.; Kumar, S. Estimating divergence times in large molecular phylogenies. *Proc. Natl. Acad. Sci. USA* **2012**, *109*, 19333–19338. [CrossRef] [PubMed]

18. Tamura, K.; Nei, M.; Kumar, S. Prospects for inferring very large phylogenies by using the neighbor-joining method. *Proc. Natl. Acad. Sci. USA* **2004**, *101*, 11030–11035. [CrossRef] [PubMed]

19. Jolley, K.A.; James, E.B.; Maiden, M.C.J. Open-access bacterial population genomics: BIGSdb software, the PubMLST.org website and their applications [version 1; peer review: 2 approved]. *Wellcome. Open. Res.* **2018**, *3*, 124. [CrossRef]

20. Bauer, A.W.; Kirby, W.M.; Sherris, J.C.; Turck, M. Antibiotic susceptibility testing by a standardized single disk method. *Am. J. Clin. Pathol.* **1966**, *45*, 493–496. [CrossRef] [PubMed]

21. Luo, Z.; Zhang, Z.G.; Hao, S.; Bai, X.H.; Gao, Q.; Feng, S.M. Isolation and Identification of the Pathogen Causing granulomas in internal organs of turbot *Scophthalmus maximus*. *J. Fish. Sci. China* **2019**, *26*, 559–568. [CrossRef]

22. Luo, Z.; Li, J.; Zhang, Z.G.; Hao, S.; Bai, X.H.; You, H.Z.; Mo, Z.L.; Feng, S.M. *Mycobacterium marinum* is the causative agent of splenic and renal granulomasin half-smooth tongue sole (*Cynoglossus semilaevis* Günther) in China. *Aquaculture* **2018**, *490*, 203–207. [CrossRef]

23. Luo, Z.; Hao, S.; Bai, X.H.; Zhang, Z.G.; Ma, Y.F.; Feng, S.M.; Zhang, D.F. Isolation, identification, and genomic analysis of *Mycobacterium ulcerans* ecovar *Liflandii* from the farmed Chinese tongue sole, *Cynoglossus semilaevis* Günther. *Aquaculture* **2022**, *548*, 737614. [CrossRef]

24. Bai, X.H.; Hao, S.; Fu, J.P.; Sun, H.C.; Luo, Z. Identification of *Mycobacterium chelonae* from Lined Seahorse *Hippocampus erectus* and Histopathological Analysis. *Fishes* **2023**, *8*, 225. [CrossRef]

25. He, S.Y.; Wei, W.Y.; Liu, T.; Yang, Q.; Xie, H.; He, Q.Y.; Wang, K.Y. Isolation, identification and histopathological study on lethal sarcoidosis of *Micropterus salmoides*. *J. Fish. China* **2020**, *44*, 253–265.

26. Zhen, C.; Pan, L.D. research progress on pathogen and histopathology of visceral sarcoidosis in fish. *Sci. Fish. Farms.* **2016**, *7*, 54–55.

27. Xiao, P.; Jiang, M.; Liu, Y.; Sun, M.; Zhang, L.; Jie, L.; Li, G.; Mo, Z. Splenic necrosis signs and pathogen detection in cultured half-smooth tongue sole, *Cynoglossus semilaevis* Günther. *J. Fish Dis.* **2015**, *38*, 103–106. [CrossRef] [PubMed]

28. Ge, M.X.; Fang, H. *Renibacterium Salmoninarum* and bacterial kidney disease of salmon (summary). *J. Hebei. Vocat. Technical. Teach. Coll.* **2003**, *17*, 51–55.

29. Liu, C.; Chang, O.Q.; Zhang, D.F.; Li, K.B.; Wang, F.; Lin, M.H.; Shi, C.B.; Jiang, L.; Wang, Q.; Bergmann, S.M. *Aeromonas schubertii* as a cause of multi-organ necrosis in internal organs of Nile tilapia, *Oreochromis niloticus*. *J. Fish Dis.* **2012**, *35*, 335–342. [CrossRef]

30. Qiu, Y.Y.; Zheng, L.; Mao, Z.J.; Chen, X.X. Isolation and identification of the causative agent and histopathology observation of white-spots disease in internal organs of *Larimichthys crocea*. *Microbiol. China* **2012**, *39*, 361–370.

31. He, X.X.; Liu, K.M.; Wang, X.Y.; Hao, S.; Jia, L.; Shao, P.; Luo, Z. Isolation, identification and histopathology of pathogen of intussusception disease in half-smooth tongue sole *Cynoglossus semilaevis*. *J. Dalian Ocean Univ.* **2022**, *37*, 19–25.

32. Kim, M.S.; Jin, J.W.; Han, H.J.; Choi, H.S.; Hong, S.; Cho, J.Y. Genotype and virulence of *Streptococcus iniae* isolated from diseased olive flounder *Paralichthys olivaceus* in Korea. *Fish Sci.* **2014**, *80*, 1277–1284. [CrossRef]

33. Pierezan, F.; Shahin, K.; Hechman, T.l.; Ang, J.; Byrne, B.A.; Soto, E. Outbreaks of severe myositis in cultured white sturgeon (*Acipenser transmontanus* L.) associated with *Streptococcus iniae*. *J. Fish Dis.* **2020**, *43*, 485–490. [CrossRef] [PubMed]

34. Chen, C.Y.; Chao, C.B.; Bowser, P.R. Comparative histopathology of *Streptococcus iniae* and *Streptococcus agalactiae*-infected tilapia. *Bull. Eur. Ass. Fish Pathol.* **2007**, *27*, 2–9.

35. Yu, X.L.; Chen, M.; Li, C.; Li, P.P.; Lei, A.Y.; Zhong, M.N.; Liang, W.W. Channel catfish *Ictalurus punctatus* outbreak infected by bacterium *Streptococcus iniae*. *J. Dalian Fish. Univ.* **2008**, *23*, 185–191.

36. Elaamri, F. First report of *Streptococcus iniae* in red porgy (*Pagrus pagrus* L.). *J. Fish Dis.* **2010**, *33*, 901–905. [CrossRef]

37. Xu, W.; Shi, H.; Wang, W.; Zhang, D.Y.; Xu, W.J.; Chai, X.J. Isolation and identification of *Streptococcus iniae* in *Larimichthys polyactis*. *Chin. J. Prev. Vet. Med.* **2022**, *44*, 725–730.

38. Pretto-Giordano, L.G.; Scarpassa, J.A.; Barbosa, A.R.; Altrão, C.S.; Ribeiro, C.G.G.; Vilas-Boas, L.A. *Streptococcus iniae*: An unusual important pathogen fish in Brazil. *J. Aquac. Res. Dev.* **2015**, *6*, 9. [CrossRef]
39. Luo, Z.; Xu, J.; Han, J.G.; Xu, Y.X.; Ma, W.T.; Feng, S.M. Isolation and identification of Pathogenetic *Streptococcus iniae* from *Selenotoca multifasciata*. *J. Huazhong Agric. Uni.* **2012**, *31*, 95–99.
40. Luo, Y.; Deng, Y.T.; Zhao, F.; Tan, A.P.; Zhang, M.C.; Jiang, L. Comparative on characteristics and pathogenicity of *Nocardia seriolae* isoalted from 9 fishes. *Microbiol. China* **2021**, *48*, 2733–2749.